The Impact of Hurricane Andrew on the Near-Surface Marine Environment in the Bahamas and the Gulf of Mexico*

L. C. BREAKER, L. D. BURROUGHS, AND Y. Y. CHAO

NOAA/National Weather Service, NMC, Washington, D.C.

J. F. CULP

NOAA/National Ocean Service, Silver Spring, Maryland

N. L. GUINASSO JR.

Texas A&M University, College Station, Texas

R. L. TEBOULLE

General Sciences Corp., Laurel, Maryland

C. R. WONG

NOAA/National Ocean Service, Silver Spring, Maryland

(Manuscript received 19 July 1993, in final form 8 June 1994)

ABSTRACT

Hurricane Andrew was a relatively small but intense hurricane that passed through the Bahamas, across the Florida Peninsula, and across the Gulf of Mexico between 23 and 26 August 1992. The characteristics of this hurricane primarily beyond its core are summarized using 1) marine observations from three National Data Buoy Center (NDBC) buoys and three Coastal-Marine Automated Network stations close to the storm track; 2) water levels and storm surge at 15 locations in the Bahamas, around the coast of Florida, and along the northern coast of the Gulf of Mexico; 3) currents, temperatures, and salinities at a depth of 11 m in the northern Gulf; and 4) spatial analyses of sea surface temperature (SST) before and after the passage of Andrew.

Sea level pressure, wind direction, wind speed, wind gust, air temperature, and the surface wave field were strongly influenced at locations generally within 100 km of the hurricane track. Maximum sustained winds of 75 m s^{-1} occurred just north of the storm track near Miami (Fowey Rocks). Significant wave height increased from 1 to 6.4 m at one NDBC buoy in the Gulf of Mexico (25.9°N, 85.9°N). A record high water level occurred at North Miami Beach. Decreases in water level occurred along the west coast of Florida with a maximum negative surge of −1.2 m at Naples. Increases in water level occurred along the Gulf coast between the Florida panhandle and Louisiana where a storm surge of +1.2 m was observed at Bay Waveland, Mississippi. Current speeds at one shallow water location along the hurricane track in the northern Gulf (28.4°N, 90.5°W) increased from ~15 to almost 140 cm s^{-1} at a depth of 11 m during passage of the storm. Finally, SSTs decreased by up to 3°C at various locations along the hurricane track.

1. Introduction

Since 1900, 15 hurricanes of intensity 4 or 5 on the Saffir/Simpson hurricane scale have affected the Florida/Gulf of Mexico region (Neumann et al. 1987). Since 1957, five hurricanes of intensity 4 or greater, including Hurricane Andrew, have affected this region. These hurricanes and their basic characteristics are summarized in Table 1.

From Table 1, Andrew's maximum sustained winds were somewhat weaker than the winds associated with the other four major tropical cyclones. Also, Andrew was the only major hurricane (Category 4 or greater) to cross the Florida peninsula and then enter the Gulf of Mexico since at least 1957.

Although Hurricane Andrew was relatively small, it was intense with a minimum central pressure of 922 mb (92.2 kPa) and maximum sustained surface winds approaching 75 m s^{-1}. This hurricane was extremely destructive and devastated portions of the Bahamas,

* OPC Contribution Number 68.

Corresponding author address: Laurence C. Breaker, NOAA/National Weather Service, NMC, Washington, DC 20233.

© 1994 American Meteorological Society

TABLE 1. Basic characteristics of major tropical cyclones.

Name	Date	Intensity[a]	Minimum pressure (mb)	Maximum sustained winds (m s^{-1})
Audrey	25–28 Jun 1957	4	940[b]	77–93[b]
Carla	3–15 Sep 1961	4	931	90[c]
Camille	5–22 Aug 1969	5	901	90[c]
Gilbert	10–17 Sep 1988	5	888	82
Andrew	16–28 Aug 1992	4	922	75

[a] Saffir/Simpson hurricane intensity scale.
[b] Estimated value.
[c] Peak value.

southern Florida, and southern Louisiana. Estimates of damage from Hurricane Andrew have reached 20–25 billion dollars in the United States alone.

Hurricane Andrew originated as a tropical wave off the west coast of Africa on 14 August 1992 and initially moved to the west at a speed of about 10 m s^{-1} (Rappaport 1994). By 16 August, Andrew became a tropical depression, and on 17 August it was classified as a tropical storm. At this stage in its development, Andrew moved rapidly to the west and then to the WNW. From 17 to 20 August, the translation speed of tropical storm Andrew decreased as it turned to the NW. By 20 August, Andrew had weakened to the point that it had a central pressure of 1015 mb; however, by 21 August, it rapidly intensified and again turned to the west. Andrew continued to intensify and by 22 August had reached hurricane strength. Hurricane Andrew reached its maximum intensity on 23 August with a minimum central pressure of 922 mb while it was just east of the Bahamas, approximately one day before reaching the east coast of Florida.

Hurricane Andrew weakened slightly over the Great Bahama Bank and reintensified just before reaching the southeast coast of Florida. The hurricane came ashore near Homestead Air Force Base (Fig. 1, approximately 5 km south of the storm track) with wind gusts of at least 78 m s^{-1} (Rappaport 1994). At this point, Andrew was moving with a speed of about 9 m s^{-1}.

After landfall, Andrew continued to move westward over the southern Florida peninsula and weakened slightly. In the four hours that it took to cross Florida, Andrew's central pressure rose to about 950 mb. After reaching the Gulf of Mexico (hereafter referred to as the Gulf), the hurricane reintensified as its direction changed from westward, to WNW, and finally to NW as it approached the coast of Louisiana. Before reaching the northern Gulf coast on 25 August, Andrew began to slow down and weaken. At this point, Andrew had maximum sustained winds of 55 m s^{-1}. It finally reached landfall in southern Louisiana on 26 August and rapidly weakened as it moved inland.

It was fortuitous that a number of National Data Buoy Center (NDBC) environmental data buoys, Coastal-Marine Automated Network (C-MAN) stations, and a Louisiana–Texas Shelf Physical Oceanography Program (LATEX) current meter mooring were located close to Andrew's track during its passage across the Bahamas and the Gulf. These data naturally take the form of time series and characterize the intensification and decay of Andrew at specific locations along its track. Additionally, we include several difference maps of satellite-derived SST to provide an alternate perspective of the ocean's response to this hurricane.

The purpose of this study is to document the impact of Hurricane Andrew on the near-surface marine environment across the Bahamas and the Gulf through observations of sea level pressure, surface winds and waves, surface air temperature, SST, water level, currents, subsurface temperature, and salinity. These observations are unique, in their entirety, and help to establish a baseline for future studies of this type. In most cases, they were acquired outside the core of the hurricane, and thus do not represent the extreme values that occurred.

2. Data sources and sensor characteristics

a. NDBC buoy and C-MAN station data

Three NDBC buoys and three C-MAN stations provided observational data for this study (Fig. 1; Table 2). Marine observations from a C-MAN station at Fowey Rocks about 25 km north of the storm track near Miami (Fig. 1) were also acquired during Andrew (Meindl 1993). Data at this location were extracted from Meindl and are included in section 3. The buoys were located near Eleuthera in the Bahamas (41016) and in the Gulf (42001 and 42003). The C-MAN sta-

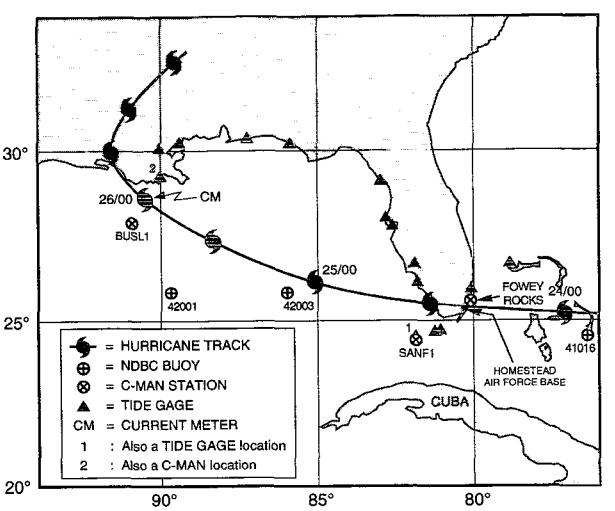

FIG. 1. Track of Hurricane Andrew plus locations of NDBC buoys, C-MAN stations, NOS tide gauge locations, and LATEX current meter.

TABLE 2. NDBC buoy and C-MAN station locations and sensor heights above mean sea level (meters) for each parameter.

Station	Latitude	Longitude	Barometric pressure	Wind speed and direction	Air temperature	SST	Wave parameters
41016	24.6°N	76.5°W	0.0	10.0	10.0	−1.0	—
SANF1	24.5°N	81.9°W	6.4	13.1	12.8	−1.5	—
42001[a]	25.9°N	89.7°W	0.0	10.0	10.0	−1.0	*
42003	25.9°N	85.9°W	0.0	10.0	10.0	−1.0	*
BUSL1	27.9°N	90.9°W	—	96.3	—	−3.0	—
GDIL1	29.3°N	90.0°W	9.1	17.7	17.1	—	—

[a] Only data on winds and surface waves from this buoy are presented in the text.
— Not included or not available.
* Surface following.

tions are SANF1, a stationary platform located offshore of Sand Key, Florida; BUSL1, an oil platform owned by Shell Offshore, Inc., which is also located offshore in the northern Gulf; and GDIL1, collocated with an NOS tide gauge at Grand Isle, Louisiana. Information about the sensor packages on the three NDBC buoys, SANF1, and GDIL1 is available from Gilhousen (1992) and NDBC (1989, 1992a,b). Information about the sensor package on BUSL1 is available from Swanson and Baxter (1989).

Table 2 gives the position of each platform and the elevation for each sensor. Descriptions of the sensors including type of sensor, sampling range, averaging frequency, and averaging period can be found in Breaker et al. (1993) and NDBC (1989).

The NDBC buoy and C-MAN station data are transmitted to the GOES geostationary satellite, which relays them to a ground receiving station. They are then routed to the National Weather Service Telecommunications Gateway, which in turn routes them to the National Meteorological Center.

b. *Coastal tide station data*

The National Ocean Service (NOS) collects, processes and analyzes water level data from approximately 190 continuously operating tide stations in U.S. coastal waters, the Great Lakes, and U.S. territories and possessions. The NOS tide stations use a stilling well float-driven gauge with an analog-to-digital recorder (ADR) that records data at 6-min intervals. Each ADR measurement is an instantaneous discrete value measured with a resolution of 0.003 m.

The NOS has implemented a Next Generation Water Level Measurement System (NGWLMS); these field units consist of a data collection platform and an acoustic sensor. The data are stored in memory and transmitted via the GOES satellite every 3 h. Measurement samples consist of 181, 1-s water level observations that are averaged and recorded at 6-min intervals. The reported measurements have a resolution 0.001 m. Additional characteristics for these instruments are given in Breaker et al. (1993).

The NOS tide stations located around the coasts of Florida and the northern Gulf are generally equipped with the ADR as well as a backup gauge. The NGWLMS system has been installed at many of these stations also with dual data collection capability. The locations, and sensor and measurement types, for the water level data presented in the next section are given in Table 3.

c. *Current meter data*

In April 1992, a number of moored current meters were deployed on the Texas–Louisiana continental shelf as part of LATEX (Guinasso 1992). Data from one particular location (mooring 14) acquired during the passage of Hurricane Andrew are reported here. Mooring 14, which was located at 90.5°W, 28.4°N (almost directly on the hurricane track) in a water depth of 48 m, is a taut subsurface mooring. An ENDECO Type 174SSM vector-averaging current meter was located at 11 m below the surface on this mooring. This instrument samples current speed and direction approximately once per second, and every 30 min records a vector-averaged current speed and direction plus instantaneous values of temperature and salinity. Data are recorded internally with a solid-state memory and are retrieved when the current meter is recovered and serviced.

d. *Satellite data*

Satellite-derived SST analyses produced by The National Oceanic and Atmospheric Administration/National Environmental Satellite Data and Information Service (NOAA/NESDIS) were used in constructing SST difference maps before and after the passage of Andrew. In particular, high-resolution regional SST analyses produced on a $1/8° \times 1/8°$ grid covering the ocean area southeast of Florida and the Caribbean, and the Gulf of Mexico were simply subtracted at each grid point. These SSTs are calculated from Advanced Very High Resolution Radiometer (AVHRR) satellite data using the NESDIS multichannel SST retrieval tech-

TABLE 3. NOS water level station locations with sensor and measurement types.

Station	Latitude	Longitude	Sensor*	Measurement type
Settlement Point, BA	26.70°N	79.00°W	ADR**	discrete
Haulover Pier, FL	25.90°N	80.12°W	ADR	discrete
Key Colony Beach, FL	24.72°N	81.00°W	ADR	discrete
Vaca Key, FL	24.71°N	81.11°W	ADR	discrete
Key West, FL	24.55°N	81.81°W	ADR	discrete
Naples, FL	26.13°N	81.81°W	ADR	discrete
Fort Myers, FL	26.65°N	81.87°W	ADR	discrete
St. Petersburg, FL	27.76°N	82.63°W	acoustic	average
Clearwater Beach, FL	27.98°N	82.83°W	ADR	discrete
Cedar Key, FL	29.15°N	83.03°W	ADR	discrete
Panama City Beach, FL	30.21°N	85.88°W	acoustic	average
Pensacola, FL	30.40°N	87.21°W	ADR	discrete
Bay Waveland Yacht Club, MS	30.33°N	89.33°W	ADR	discrete
Grand Isle, LA	29.26°N	89.96°W	ADR	discrete
New Canal, LA	30.03°N	90.11°W	ADR	discrete

* This sensor provided the water level measurements presented in this study.
** ADR = Analog-to-digital recorder.

nique (e.g., Walton 1988). These analyses are produced twice per week using observations composited over an approximate 3½-day period. During periods of cloud cover, these analyses relax back to previous cloud-free values at the affected grid points. For additional information, see McClain et al. (1985).

3. Results

a. *Meteorological observations from the NDBC buoys and C-MAN stations*

Sea level pressure, wind speed and direction, wind gust, air temperature, and SST data were acquired at six locations close to the track of Hurricane Andrew (Fig. 1; Table 2) with the exception of BUSL1 (27.9°W, 90.9°W) where sea level pressure and air temperature were not routinely available and at GDIL1 where SST was not available. The barometric pressure was recorded at BUSL1 but was not transmitted over the C-MAN network. The minimum pressure at this platform was 999 mb (G. Forristall 1993, personal communication). Sea level pressure, wind speed and direction, and water level are reported for GDIL1. The approximate distance of each buoy or C-MAN station from the hurricane track is given in Table 4. Time series of sea level pressure, wind direction, wind speed, wind gust, air temperature, SST and sensible heat flux are presented for each location in Fig. 2 (except for GDIL1). These parameters, with the possible exception of wind gust and sensible heat flux, are self-explanatory.

A wind gust corresponds to a brief increase in wind speed (usually less than 20 s in duration) followed by a lull or slackening in wind speed (Huschke 1959). Wind gust as it is measured at the NDBC buoys and C-MAN stations represents the highest mean wind speed recorded for any 8-s window. For the BUSL1 station, wind gust represents the highest mean wind speed recorded for any 3-s window. In Fig. 2, data on wind gusts have only been included for the period surrounding the peak winds associated with the passage

TABLE 4. Selected statistics from NDBC buoys and C-MAN stations associated with Hurricane Andrew.

Station—to the left (L) or right (R) of the storm track	Distance from track (km)*	Min sea level pressure in mb	Max wind speed ($m\ s^{-1}$)	Max wind gust ($m\ s^{-1}$)	Estimated drop in air temp. (°C)	Maximum sensible heat flux ($W\ m^{-2}$)	Maximum significant wave height (m)
41016 (L)	78	1007.9	14.7	18.1	2.0	68	—
SANF1 (L)	133	1010.2	15.6	17.9	4.0	183	—
42001 (L)	208	—	12.3	—	—	—	4.3
42003 (L)	63	997.4	23.2	30.6	3.5	183	6.4
BUSL1 (L)	97	**	26.6	32.3	**	**	—
GDIL1 (R)	85	1005.2	24.7	—	4.9	—	—

* Estimated distance to closest point of approach.
** Not available from C-MAN network; see text for additional information.
— Not available.

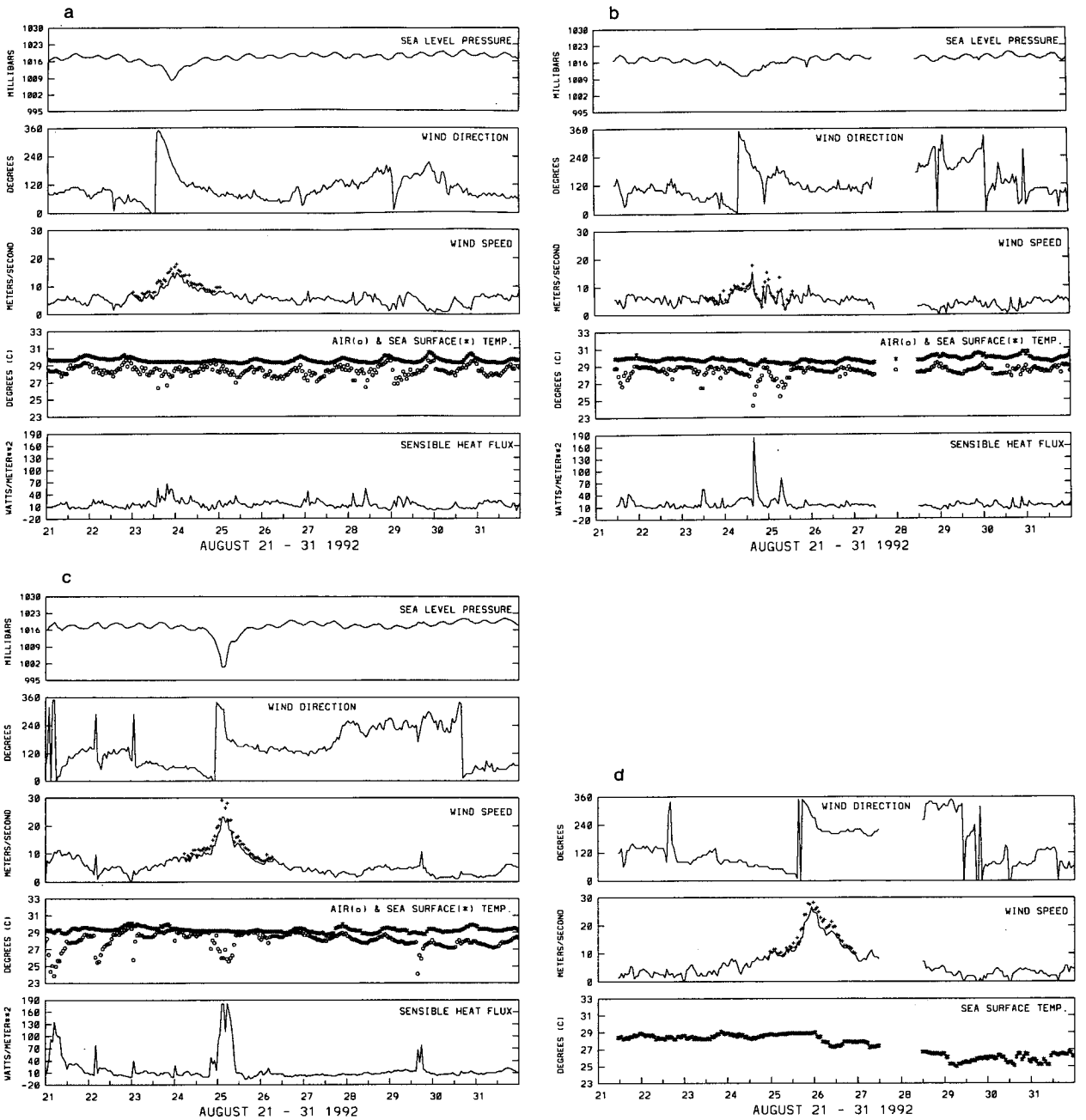

FIG. 2. Hourly time series for sea level pressure, wind direction, wind speed, wind gust, air, and SST, and sensible heat flux for: (a) 21 August 1992 through 31 August 1992 for NDBC buoy 41016 (24.6°N, 76.5°W), (b) 21 August 1992 through 31 August 1992 for C-MAN station SANF1 (24.5°N, 81.9°W) (Gap on 27 and 28 August is due to missing data.), (c) 21 August 1992 through 31 August 1992 for NDBC buoy 42003 (25.9°N, 85.9°W), and (d) 21 August 1992 through 31 August 1992 for C-MAN station BUSL1 (27.9°N, 90.9°W). (Sea level pressure and air temperature were not available at this location, and since air temperature was not available, sensible heat flux could not be calculated.) Wind gusts are plotted above wind speeds for ±24 h of the wind speed maximum in each case.

of the hurricane (i.e., ±24 h of the maximum value of wind speed).

The sensible heat flux (SHF) is a derived quantity calculated from the sea–air temperature difference and the wind speed. A standard bulk aerodynamic formulation was used (e.g., Kraus 1972),

$$\mathrm{SHF} = c_p \rho_a \zeta (T_0 - T_{10}) U_{10},$$

where c_p is the specific heat of air, ρ_a is the air density, ζ is the drag coefficient (2.0×10^{-3} is used here), T_0 and T_{10} are the SST and the air temperature at a height of 10 m, and U_{10} is the wind speed at 10 m. When the

SHF is positive, a transfer of heat from the ocean to the atmosphere is indicated, and vice versa. The SHF represents one source of energy for hurricane development and maintenance.

In addition to the distances between measurement location and the hurricane track, extreme values for sea level pressure, wind speed, wind gust, SHF, and significant wave height are included in Table 4. Also, the estimated maximum decrease in air temperature during the storm period is given. The changes in SST were usually very small (<1°C) during the periods associated with the hurricane per se. A gradual but significant decrease (~ −3°C) did occur at BUSL1, however, during the first five days following the hurricane (Fig. 2d).

Table 4 indicates a weak dependence on distance from the hurricane for the extreme values of sea level pressure, wind speed, and wave height. (Hurricane wind speeds also depend on the central pressure of the storm and whether the observing site is to the left or right of the storm's track.) The lowest sea level pressure (997 mb) and the highest wind gust (32 m s^{-1}) were recorded at buoys 42003 and BUSL1, respectively, which were only about 63 and 97 km from the track.[1] Although the highest wind reported through the C-MAN network at BUSL1 in the northern Gulf was 27 m s^{-1}, continuous recordings on the platform from additional anemometers showed maximum winds of 29.5 m s^{-1} at another location on the platform and 34.8 m s^{-1} at a third location. An aircraft reconnaissance flight reported wind speeds in the storm near the surface as high as 50 m s^{-1} (G. Forristall 1993, personal communication). Even the maximum wind gust at BUSL1, however, did not approach the maximum winds reported for Hurricane Andrew elsewhere along its path (e.g., wind gusts of up to 78 m s^{-1} were reported near Homestead Air Force Base in South Florida and a maximum sustained wind of 75 m s^{-1} at Fowey Rocks, just north of the storm track). Distance from the hurricane plus the fact that the wind observations were acquired at 10 m, well below the level where wind maxima usually occur for hurricanes, most likely account for these differences. Also, these measurement sites (except for GDIL1) were located to the left of the storm track where the large-scale circulation acts to reduce the winds observed at a fixed location.

Marine observations were also acquired at a C-MAN station located approximately 25 km north of the storm track at Fowey Rocks (25.6°N, 80.1°W) on the east coast of Florida (already referred to earlier in this section). Because these data were not available to us in their entirety, we summarize the results of Meindl (1993) for this location. Maximum winds of 75.5 m s^{-1} (at a height of 44 m) and a minimum sea level pressure of 967 mb (at a height of 29 m) were recorded at 0800 UTC on 24 August 1992. At this time, the anemometer mast failed. These observations were acquired in the northern eyewall of the hurricane and represent the most extreme values recorded by any fixed marine observing system during Hurricane Andrew. The strongest winds probably occurred after this instrument failed because the storm continued to intensify after it passed Fowey Rocks (E. Rappaport 1993, personal communication).

A sequence of surface analyses show the proximity of the C-MAN and buoy data from certain stations listed in Table 2 to Hurricane Andrew as it moved from the Atlantic, across southern Florida, and into the Gulf of Mexico (Fig. 3). These analyses show streamlines and isotachs from the latest version of NMC's Global Data Assimilation system (Parrish and Derber 1992). The station data that are superimposed show surface winds, sea level pressures, air temperatures, and SSTs plotted in standard meteorological format (WMO 1981) except that the wind flags are plotted every 10 m s^{-1} instead of every 5 m s^{-1}.[2] Overall, the level of agreement between the analyzed winds and the observed winds is excellent.

Air temperatures for the three locations dropped significantly in each case. Since SST showed almost no change during the period of maximum winds, it was the decrease in air temperature (plus the increase in wind speed) that primarily contributed to the large increases in SHF.

b. Surface waves from the NDBC buoys

Wave conditions were recorded at NDBC buoys 42001 and 42003 in the Gulf of Mexico during the passage of Hurricane Andrew (Fig. 1). Minimum distances from buoys 42003 and 42001 to the hurricane track were approximately 63 and 208 km, respectively (Table 4).

Time series plots of the wind speed, wind direction, significant wave height, and peak period at buoys 42003 and 42001 are shown in Fig. 4a and 4b, respectively. The peak period corresponds to that wave frequency that is associated with the maximum spectral energy density.

At buoy 42003 (Fig. 4a), a gradual increase in wind speed occurred between 23 August at 0300 UTC and 24 August at 2100 UTC. The wind direction was approximately NE. Noticeable increases in wave height and wave period did not begin until 24 August (0000 UTC) when the wind speed had reached ~8 m s^{-1}. A sharp increase in the wind speed, wave

[1] The anemometers at BUSL1, however, were mounted at a height of approximately 94 m, and so it was difficult to compare the wind speeds at this location with those at the other locations (since no adjustment to a standard height of 10 m was made).

[2] The station farthest to the west in the upper-right panel, and the two lower panels, had only wind and SST available in real time.

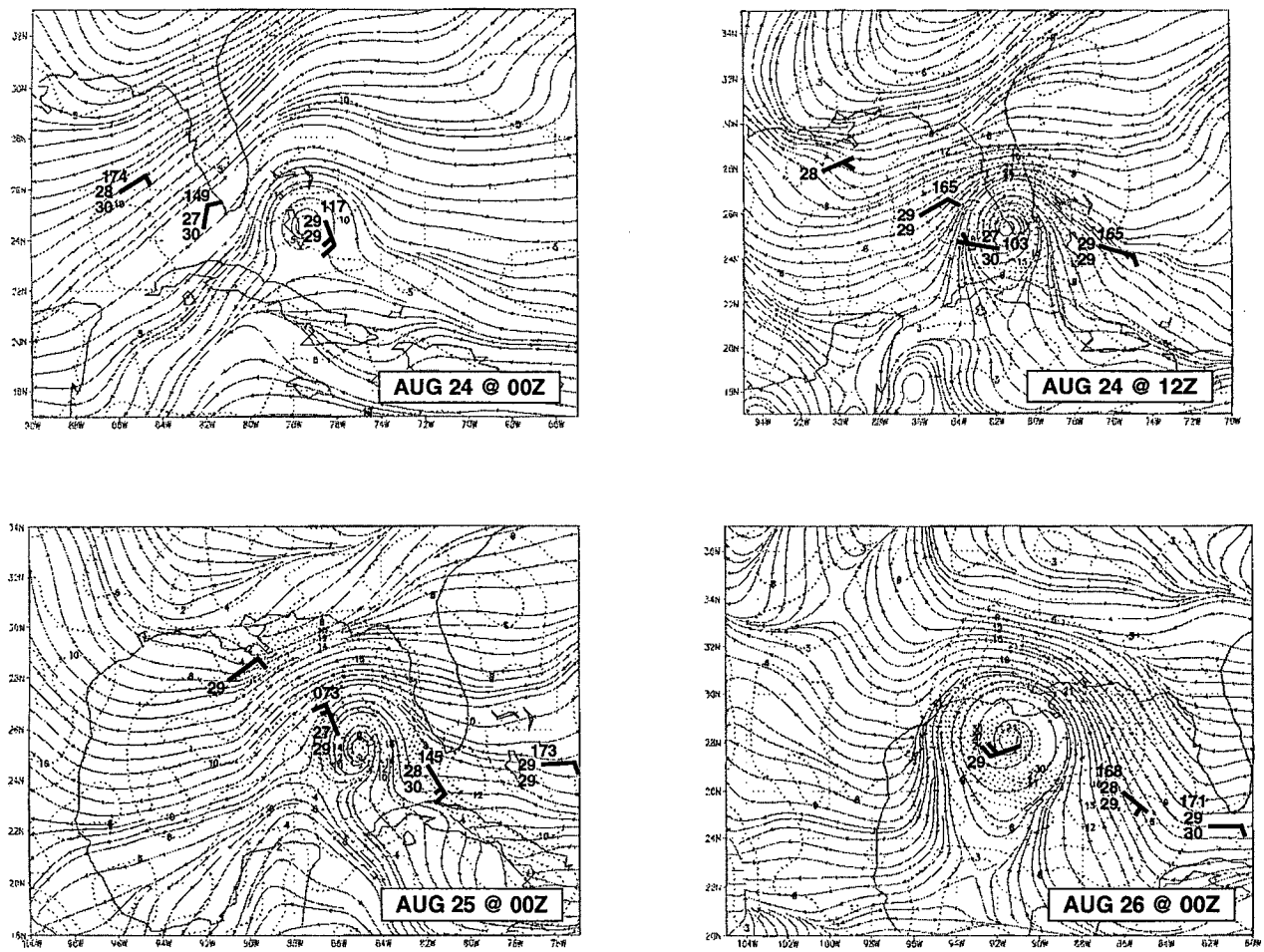

FIG. 3. Sequence of surface wind speeds (isotachs) and streamlines for (a) 0000 UTC 24 August, (b) 1200 UTC 24 August, (c) 0000 UTC 25 August, and (d) 0000 UTC 26 August.

height, and wave period occurred on 24 August (~2100 UTC) and reached their maximum values on 25 August (~0300 UTC) when the hurricane was closest to the buoy. During this period, the wind speed increased from 10 to 23 m s^{-1}, the wave height increased from just under 2 m to more than 6 m, the wave period increased from about 7 to 17 s, while the wind direction changed from N to NW. It took approximately nine hours for the wind speed and the wave height to return to their previous values (~10 m s^{-1} and ~2 m, respectively). Beyond that point, wind speed and wave height decreased more slowly. Conversely, the peak wave period decreased rapidly to ~7 s immediately following its maximum value during the first six hours on 25 August. It remained in that range until 0600 UTC on 26 August when it rapidly increased to 10 s by ~2100 UTC and then started to decrease again. The wind direction also changed rapidly from NW to S during the time of a sharp decrease in wave height and then remained essentially constant from the SE until about 1200 UTC on 27 August.

At buoy 42001, a gradual but fluctuating increase in wind speed began on 23 August (~0000 UTC). The wind direction was essentially NE. Increases in wave height and wave period, however, did not begin until ~1200 UTC on 24 August. A relatively sharp increase in wave height and wave period occurred on 25 August (~0900 UTC) and reached their extreme values three hours later as the hurricane reached its closest point of approach to the buoy. During this period, the wave height increased from slightly less than 2 m to more than 4 m, the wave period increased from 7 to 17 s, and the wind direction changed from N to NW. The wind speed, however, continued to gradually increase to its maximum value (~12 m s^{-1}) 6 h after the occurrence of the maximum wave height, and then slowly decreased. The wind direction during this time was essentially from the SW. It took about 6 h for the wave height to return from its peak value to its previous

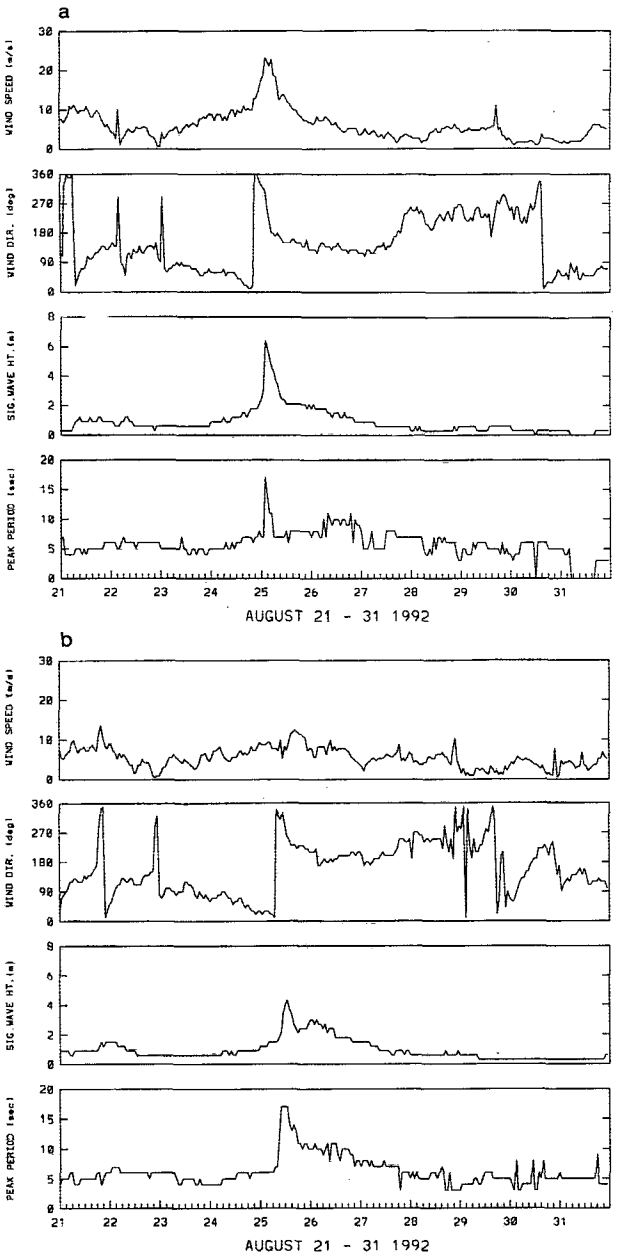

FIG. 4. Hourly time series for wind speed and direction, significant wave height, and peak period for: (a) NDBC buoy 42003 (25.9°N, 85.9°N) for 21 August 1992 through 31 August 1992. (b) NDBC buoy 42001 (25.9°N, 89.7°W) for 21 August 1992 through 31 August 1992. Steplike appearance for significant wave height and peak period is due to prior truncation of the data.

value of 2 m. At the same time, the wave period decreased to 10 s, and the wind direction changed from NW to SW. We note that the wave height increased again to a second maximum of 3 m on 26 August (~0000 UTC) and decreased to 2 m approximately 12 h later.

The variation of spectral energy density and mean wave direction at buoys 42003 and 42001 as a function of frequency and time between 1200 UTC on 24 August and 0000 UTC on 27 August is portrayed in Fig. 5. At the times when the hurricane was closest to the buoys, the spectral energy density reached a maximum. The frequency at this spectral peak was 0.06 Hz, which corresponds to a wave period of 17 s. The lowest frequency with appreciable energy was 0.05 Hz or even slightly lower (with a wave period of at least 20 s). Whereas most of the wave energy at buoy 42003 was confined to frequencies between 0.1 and 0.2 Hz (wave periods of 5–10 s), the corresponding frequency range at buoy 42001 was 0.08 to 0.14 Hz (wave periods of 7–13 s). Thus, the waves at 42001 had wave periods that were longer and were concentrated in a narrower range of frequencies than those at 42003.

It is of interest to examine the partitioning of the local wind waves and swell during wave evolution at the two buoy locations, and to determine why significant wave heights at buoy 42001 reached their highest values prior to the maximum in wind speed. Considering the time series in wind direction (Fig. 4) and wave direction at buoy 42003 (Fig. 5; upper panel), it is apparent that waves at buoy 42003, up to ~0600 UTC 25 August, were generated by the hurricane, as

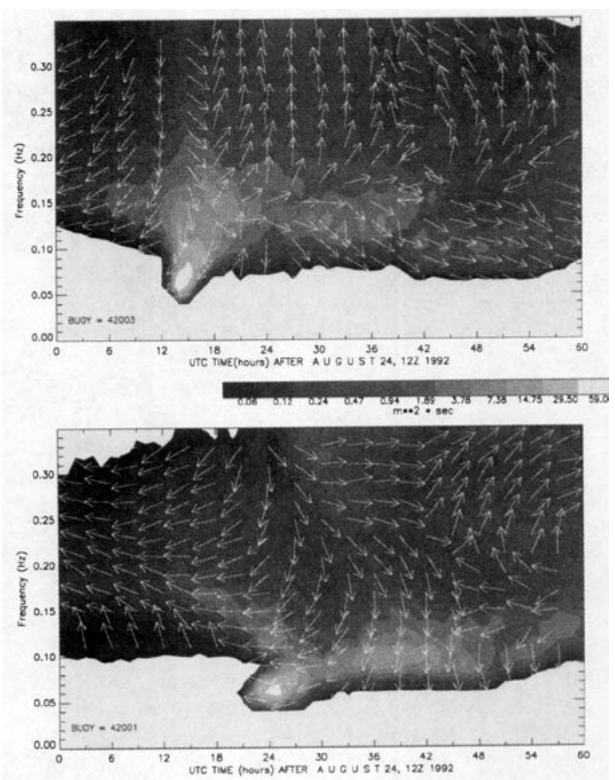

FIG. 5. Wave spectra for the period 1200 UTC 24 August to 1200 UTC 26 August at NDBC buoy 42003 (25.9°N, 85.9°W) and buoy 42001 (25.9°N, 89.7°W). Units for wave spectra are m^2 sec^{-1} (applicable to the scale located between upper and lower panels). The arrows indicate the mean wave directions for the various frequency components.

the wind direction shifted from ~NE to ~NW during the hurricane's approach. As the hurricane moved away from the buoy, the wind direction shifted to southerly. While the high-frequency waves were still driven by the local winds, waves with frequencies lower than ~0.15 Hz were essentially swell that arrived from the ~NW. In contrast, the major portion of the wave energy at buoy 42001 was due to the arrival of swell. Only waves of frequencies higher than ~0.2 Hz were influenced by the local winds. Three different directional wave groups can be identified at the higher frequencies. The first occurs prior to ~1500 UTC 25 August. The second occurs after ~0600 UTC 26 August. The first group is associated with winds from ~NE to ~NW, whereas the second is essentially southerly. The third group occurs between the first two and has a dominant westerly component. This group appears to be transient in nature. The easterly waves with a 17-s peak period (0.06 Hz), which produced the highest energy levels at ~1200 UTC 25 August are most likely components of the swell propagated from 42003. For a 17-s period wave, the group velocity is ~14 m s^{-1}, and over a period of 9 h, it propagates ~440 km, approximately the distance between the two buoys.

c. Water levels

The predicted tides were computed using standard harmonic analysis and tide prediction algorithms (Shureman 1958; Zetler 1982). Elevations are relative to Mean Lower Low Water (MLLW) at each station. Storm surges were generated by subtracting the predicted water levels (i.e., the astronomical tides) from the observed water levels. Table 5 shows the extreme water level elevations recorded during Hurricane Andrew compared with the historical extremes at each station[3] and the extreme values of storm surge. The time series plots of hourly storm surge are shown in Fig. 6.

Early on 24 August 1992, Hurricane Andrew left the Bahamas and crossed the Straits of Florida. No discernible effect on water level was observed at the Settlement Point tide station (Fig. 6a). This was due to one or more factors: 1) the storm intensity was somewhat weaker over the Great Bahama Bank, 2) the Settlement Point tide gauge is located in a sheltered area on Grand Bahama Island (GBI), or 3) the orientation of GBI may have blocked most of the storm surge generated in this area. The center of Andrew crossed the southeast coast of Florida at approximately 0900 UTC 24 August 1992. The tide station at Haulover Pier, in North Miami Beach, located approximately 50 km north of the landfall point, recorded a maximum water level of 1.65 m above MLLW, which exceeded the historical maximum by 0.22 m (Table 5). The maximum storm surge of 0.79 m above MLLW (Fig. 6; Table 5) occurred at 0900 UTC near the expected time of high water. The pier and the tide gauge sustained considerable damage from the hurricane. Although data transmissions ceased at ~0900 UTC on 24 August 1992, subsequent data were acquired and retrieved from internal storage.

Data received from NOS tide stations in the Florida Keys south of the hurricane track show that storm effects on water levels were small (Fig. 6a). The deep water exposure of these stations undoubtedly contributed to this lack of response. The records at Vaca Key and Key West do, however, reveal increased oscillatory behavior following the passage of Andrew.

Along the Florida west coast, negative elevations in water level were observed near the hurricane track while the storm center was still located over land (Fig. 6b). Naples, which was the closest station to the eye of the hurricane, recorded a drop in elevation that exceeded the lowest historical elevation by 0.13 m. The drop in water level occurred at the time of predicted high water, resulting in a negative surge of −1.21 m. A maximum positive surge of approximately +0.4 m was observed after the passage of Andrew.

A comparison of Clearwater Beach, located on the Gulf coast, and St. Petersburg, located on the western shore of Tampa Bay, shows the varying effects of the hurricane at two locations at approximately the same latitude (Fig. 6b). Clearwater Beach had a more intense negative surge (−0.62 m) and lower water level elevations than St. Petersburg, which experienced a maximum negative surge of −0.34 m. Although St. Petersburg was actually closer to the storm center, the restricted flow within Tampa Bay resulted in a smaller response. All of the NOS tide gauges along the west coast of Florida reached a maximum positive surge of approximately +0.5 m within the first 24 h after the passage of Andrew.

After Hurricane Andrew entered the Gulf, increases in water level and surge were observed along the Florida panhandle (Fig. 6c). Storm surge plots for the Florida panhandle also show a secondary maximum on 27 August 1992.

After landfall in Louisiana, Hurricane Andrew proceeded north and then northeast, and passed to the west of Lake Pontchartrain (30.2°N, 90.1°W). The tidal records at New Canal, on the eastern shore of Lake Pontchartrain, indicate that highest water and maximum surge did not occur until the evening of 26 August 1992 (Fig. 6c). High water and surge were sustained through 27 August 1992 at this location.

Hourly time series of sea level pressure, wind speed, wind direction, observed and predicted water levels, and storm surge at Grand Isle, Louisiana, are shown in Fig. 7a for 21 August 1992 through 31 August 1992. The peak winds are closely associated with the minimum pressure at this location while there is a lag of

[3] The historical record depends on the installation date for each station and on any gaps that may have occurred during the period of data acquisition. For further information see NOS (1990).

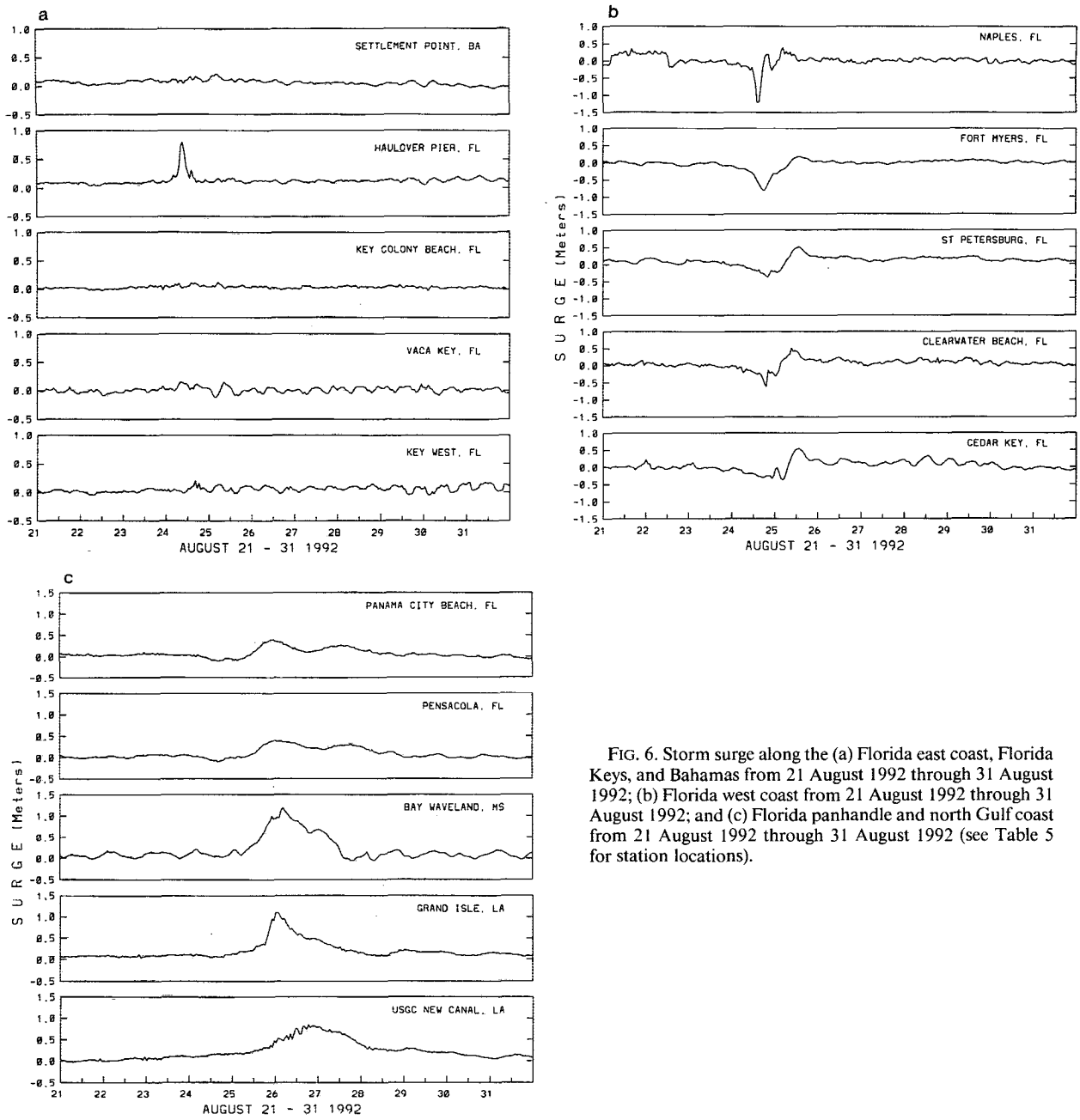

FIG. 6. Storm surge along the (a) Florida east coast, Florida Keys, and Bahamas from 21 August 1992 through 31 August 1992; (b) Florida west coast from 21 August 1992 through 31 August 1992; and (c) Florida panhandle and north Gulf coast from 21 August 1992 through 31 August 1992 (see Table 5 for station locations).

1–2 h in the peak surge. At the same time that the winds began to decrease, the wind direction changed from ENE to SW, which indicated that Andrew had passed from South to North of Grand Isle. A maximum surge of 1.1 m occurs at approximately 0000 UTC 26 August. The decrease in sea level pressure is about 10 mb, which corresponds to a pressure setup of approximately 0.1 m. Thus, only about 10% of the increase in water level at Grand Isle can be accounted for by the decrease in pressure; the other 90% was due to the combined effects of wind-driven transport, wave setup, and precipitation.

The water level data presented here are referenced to datums that have been established by NOS. However, higher water levels were observed closer to Andrew's track, but these were not referenced to any established datums. For example, a maximum still water elevation of 4.9 m was observed on the west side of Eleuthra in the Bahamas (E. Rappaport 1993, personal communication). A maximum water level of 5.2 m was observed at one location along the shore of South Biscayne Bay. On the west coast of Florida, just south of the location where the eye of the hurricane passed, a maximum water level of 3.5 m was estimated from

TABLE 5. Observed extreme water level elevations above MLLW (meters) plus historical extreme water levels, and extreme storm surge elevations relative to the astronomical tide.

	Hurricane Andrew elevation above MLLW (meters)		Historical extreme elevation above MLLW (meters)		
Station	Date/Time	Elev	Date	Elev	Surge
Settlement Point, BA	*		Jan 87	1.38	
Haulover Pier, FL	24 Aug 0854	1.65	Nov 84	1.43	
	24 Aug 0900 (S)**		Oct 90		0.79
Key Colony Beach, FL	*			1.05	
Vaca Key, FL	24 Aug 1212	0.48	Oct 74	0.80	
	24 Aug 0800 (S)				0.15
Key West, FL	*		Sep 65	1.21	
Naples, FL	24 Aug 1442	−0.84	Mar 88	−0.71	
	24 Aug 1400 (S)				−1.21
	25 Aug 1424	1.11	Dec 72	1.87	
	24 Aug 0400 (S)				0.38
Fort Myers, FL	24 Aug 1812	−0.32	Jan 72	−0.62	
	24 Aug 1700 (S)				−0.80
	25 Aug 1730	0.65	Nov 88	1.47	
	25 Aug 1300 (S)				0.18
St. Petersburg, FL	24 Aug 2206	−0.28	Jan 77	−0.69	
	24 Aug 1900 (S)				−0.34
	25 Aug 1254	1.15	Aug 85	1.97	
	25 Aug 1300 (S)				0.51
Clearwater Beach, FL	24 Aug 1912	−0.61	Jan 77	−0.73	
	24 Aug 1900 (S)				−0.62
	25 Aug 1254	1.37	Aug 85	1.86	
	25 Aug 0900 (S)				0.52
Cedar Key, FL	24 Aug 2212	−0.36	Sep 47	−1.24	
	25 Aug 0400 (S)				−0.27
	25 Aug 1518	1.67	Jun 72	2.48	
	25 Aug 1300 (S)				0.66
Panama City Beach, FL	25 Aug 1324	0.83	Oct 92	1.02	
	25 Aug 1800 (S)				0.41
Pensacola, FL	26 Aug 1400	0.81	Sep 26	2.69	
	26 Aug 0200 (S)				0.39
Bay Waveland, MS	26 Aug 1436	1.37	Jan 83	2.03	
	26 Aug 0400 (S)				1.19
Grand Isle, LA	26 Aug 0054	1.16	Oct 85	1.46	
	26 Aug 0000 (S)				1.11
New Canal, LA	26 Aug 2036	0.96	Jan 83	1.08	
	26 Aug 1800 (S)				0.84

Notes: MLLW is mean lower low water, times are UTC. Storm surge = observed minus predicted elevations. *Maximum water level elevations not significantly affected by Hurricane Andrew. **(S) indicates the time of extreme storm surge.

debris lines. Finally, maximum water levels in the range of 2.4 to 3.0 m were estimated along the coast of Louisiana.

d. Current meter observations

The current meter attached to LATEX mooring 14 (Fig. 1) at 11 m below the surface responded dramatically to the passage of Hurricane Andrew (Fig. 7b). Typical current speeds at this location averaged about 9 cm s^{-1} and did not exceed 19 cm s^{-1} during the prestorm period from 21 to 24 August. The eye of the storm passed about 10 km east of the mooring at about 2300 UTC 25 August. Current speeds began increasing shortly after 1200 UTC on the 25th with a direction of flow to the southwest approximately parallel to the local bathymetric contours. Current speeds of 134 cm s^{-1} were reached as the eye passed overhead, and current speeds greater than 100 cm s^{-1} to the southwest were maintained for 3 h after passage of the eye, although the direction of the prevailing wind had changed such that it opposed the current. The peak current speeds are delayed by approximately 1 h in comparison to the peak winds at BUSL1. Since the winds were not acquired at exactly the same location as the current meter data,[4] it is not possible to precisely estimate the response time of the upper ocean to wind forcing at the surface.

[4] The winds were acquired 68 km southwest of the current meter location, the closest location where wind data were available.

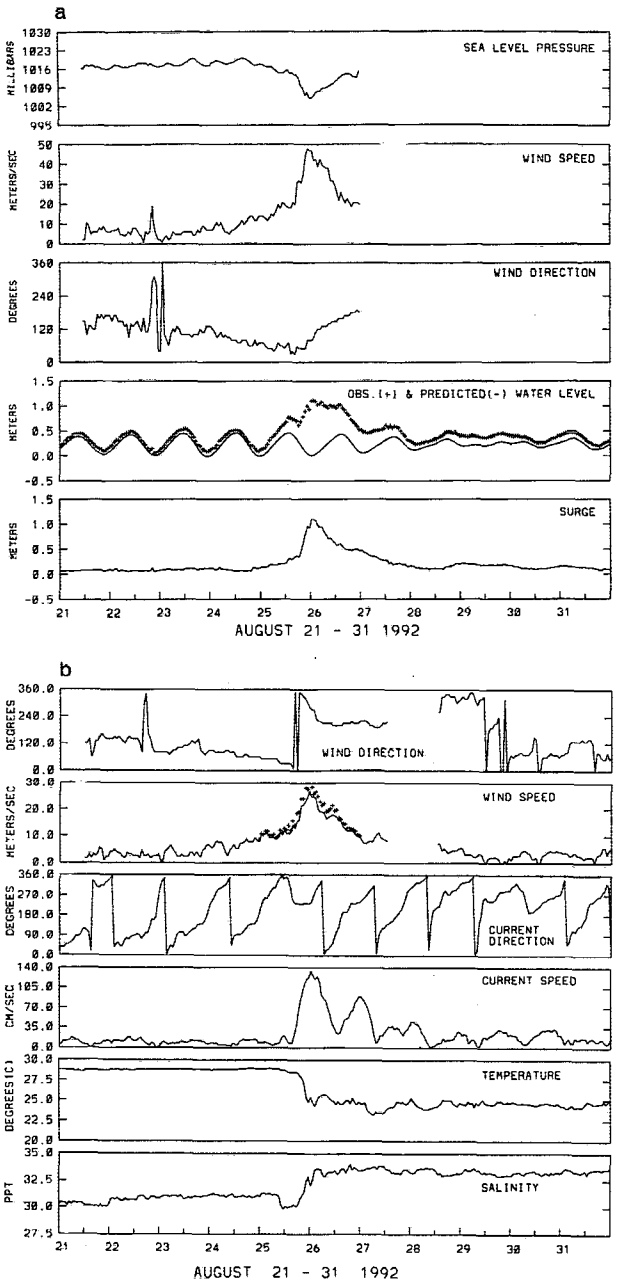

FIG. 7. Hourly time series of sea level pressure, wind speed, wind direction, observed and predicted water levels, and storm surge at (a) Grand Isle, Louisiana, for 21 August 1992 through 31 August 1992 (Data truncated at 27 August 1992 due to equipment failure immediately following the arrival of Hurricane Andrew.) and (b) BUSL1 C-MAN station (27.9°N, 90.9°N) and the corresponding time series of current speed and direction, temperature, and salinity at a depth of 11 m at current meter (CM) location 28.4°N, 90.5°W for 21 August 1992 through 31 August 1992. The BUSL1 and CM locations are 68-km apart.

Following passage of the eye, currents rotated clockwise in a series of oscillations that continued for the next 4 to 5 days. The period of these oscillations is approximately 24 h, which is consistent with an inertial response at this latitude (i.e., 28°N). In more detail, current speeds decreased rapidly from their maximum value at about 0000 UTC 26 August and reached a minimum value at about 1200 UTC on the same day. A second maximum of 88 cm s^{-1} occurred at 0000 UTC 27 August, producing strong flow to the SW. During and following the passage of Hurricane Andrew over mooring 14, the temperature at 11 m decreased (~ -4°C) and the salinity increased ($\sim +2.5$ ppt; Fig. 7, bottom two panels).

e. *Satellite SST differences*

Significant decreases in SST occurred between 18 and 29 August 1992 for the Atlantic region (18°–32°N, 70°–85°W) shown in Fig. 8. Since the hurricane did not pass through this region until 24 August (Fig. 1), most of this change occurred between 24 and 29 August. SSTs were generally isothermal prior to the passage of Andrew with temperatures off the east coast of Florida and in the Bahamas averaging around 30°C (not shown), which is about 1°C warmer than climatology for this area (Robinson et al. 1979). SSTs decreased by as much as 2°C in areas north of Andrew's track (Fig. 8). The appearance of pockets or local areas of cooler water rather than a more continuous band of cool water may have been due to cloud cover that prevented the satellite from sensing the ocean surface in certain areas.

Prior to the storm, SSTs in the Gulf also tended to be isothermal with temperatures averaging close to 30°C, which is generally 0.5°–1.0°C higher than climatology. The greatest cooling between 18 and 29 August 1992 (up to −2°C), often, but not always, occurred just north of (i.e., to the right of) the hurricane track (Fig. 8). In the northern Gulf, cooling of −1 to −2°C also occurs to the *left* of the storm track. This cooling is corroborated by a gradual decrease in SST of up to −3°C following the storm at BUSL1 (Fig. 2d). Again, the cooling is not continuous along the track but appears as pockets of cooler water, which, as indicated before, may have been due to intermittent cloud cover. Also of interest in this case is the rather linear boundary of no change (i.e., the 0°C contour) that extends from Yucatan, Mexico, to the south Texas coast (25°–26°N).

4. Discussion

It was initially surprising that SST at each of the buoys and at one of the C-MAN stations remained virtually unchanged during the passage of Hurricane Andrew. However, each of the measurement sites except one (GDIL1) was located south, or to the left, of the hurricane track. Both observations and theory indicate that maximum reductions in SST occur to the right of hurricanes (e.g., Black et al. 1988; Black 1983; Price 1981; Chang and Anthes 1978). Also, Hurricane

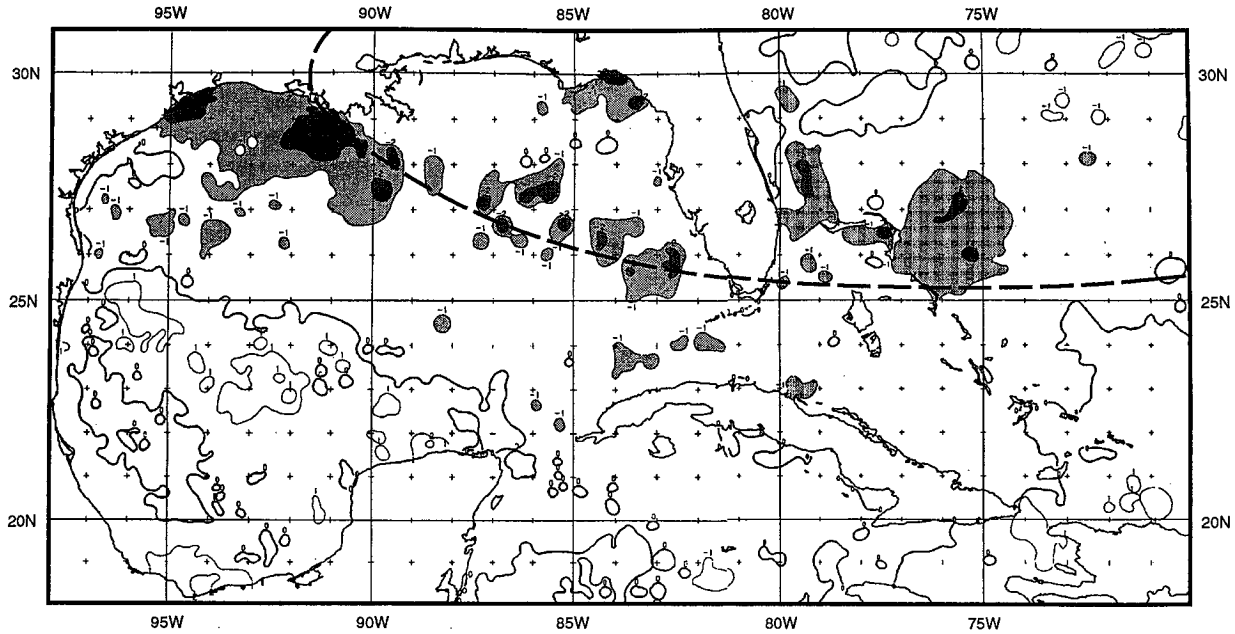

FIG. 8. Satellite-derived differences in SST (°C) between 29 August 1992 and 18 August 1992 for the region off the Florida east coast and the Bahamas, and the Gulf of Mexico. Light shading indicates SST anomalies of 0° to −1°C, and the darker shading indicates SST anomalies of −1° to −2°C.

Andrew was a relatively small [maximum winds occurred 15–20 km from the center of the storm (E. Rappaport 1992, personal communication)], rapidly moving storm and consequently might have been expected to have less effect on SST than a larger, slower-moving storm, particularly at sites located well beyond the radius of maximum winds. To the right of the storm the maximum reductions in the satellite-derived SSTs were approximately 2°C (Fig. 8). At GDIL1, SST dropped 1.7°C between 25 August at 0900 UTC and 26 August at 2300 UTC, while air temperature dropped 4.9°C from 25 August at 0900 UTC to 25 August at 2200 UTC, when the maximum wind occurred (not shown). The apparently strong response in temperature (a decrease of ~4°C) and salinity (an increase of 2–3 ppt) at the current meter mooring most likely reflects 1) its close proximity to the storm track, 2) a shallow water depth (48 m), and 3) that hurricane-forced vertical mixing, entrainment, and upwelling of colder and higher salinity water were important at the level of the current meter (11 m). Also, the current meter was located in an area where the SST anomaly was less than −2°C, an area that was located to the *left* of the storm track (Fig. 8). Finally, although a rapid decrease in SST was not observed at BUSL1 during the passage of Andrew, a gradual decrease of at least 3°C did occur over the next six days, generally consistent with the satellite-observed decrease in SST at this location.

Since the NDBC buoys were located to the left of the hurricane track, the wind speed and wave height at these locations were expected to be less than those to the right of the track at equivalent distances from the center of the storm. Winds from the NE with a relatively long duration and fetch had produced waves with periods of 5–10 s and wave heights of 1 to 2 m. The wave height and period at the buoy locations increased rapidly at the storm's closest point of approach. After the storm's departure, wave heights and periods decreased rapidly. However, the process of wave decay was complicated by the arrival of swell from various directions. As the center of the storm moved northwestward, winds turned southerly in the area where these buoys were located. A new wave system was produced by these relatively low speed but long fetch winds. This secondary wave system contributed to the rather slow decay in wave period and wave height well after the storm left the area.

Water levels provide another indication of the somewhat spatially restricted influence of Hurricane Andrew. Andrew had little effect on water levels at most tide stations along the east coast of Florida down to the Florida Keys. The only tide gauge where a significant increase in water level was observed was about 50 km north of the storm track at North Miami Beach. However, land survey information from the Hurricane Response Team of the Army Corps of Engineers indicated much higher storm surges near the location where the eye made landfall (A. Garcia 1993, personal communication).

The marked decrease in water levels along the west coast of Florida was greatest near the storm track and diminished rapidly with distance to the north. At Na-

ples, on the west coast of Florida, a record decrease in water level was observed. The negative surge was caused by surface winds that transported water away from the coast while the eye of the hurricane was still over land. After Andrew passed into the Gulf, maximum water levels occurred along the west coast of Florida caused by surface winds that transported waters toward the coast.

Increased water levels were observed along the Florida panhandle westward to Louisiana, but in no case did they exceed historical maxima. Water levels were elevated for several days during and after the storm that resulted in an extended surge from western Florida through eastern Louisiana. The direction of the sustained winds along a shallow shelf together with the physical barrier effect of the Mississippi Delta caused an accumulation of water along the northern Gulf coast and the Mississippi Sound areas. A secondary maximum in storm surge was observed along the Florida panhandle on 27 August.

Hurricane Andrew made its second landfall in south-central Louisiana at 0830 UTC 26 August 1992. The tide station closest to the hurricane was at Grand Isle. A lower storm intensity, together with low tide at the time of landfall, limited water elevations and storm surges from exceeding historical maxima along the Gulf coast. However, tide stations south of Grand Isle, at Cocodrie and South Pass (not shown), were inundated and ceased operation before the peak of the storm. Incomplete water level records indicated that historical maxima had been exceeded at both locations.

Water levels in Lake Ponchartrain were influenced by the passage of Andrew. Southeast winds from Andrew as the storm made landfall in Louisiana forced Gulf waters into Lake Ponchartrain. Higher water levels in the lake were prolonged and were most likely due to the combined effects of 1) higher water levels initially, 2) surface winds that were favorable for maintaining higher water levels in the lake, and 3) runoff into the lake from the heavy rains that ensued. These waters were subsequently released back into the Gulf within about four days after the passage of Andrew.

With regard to the current meter observations, the very high current speeds resulting from the passage of Andrew were most likely produced by 1) flow driven by the local wind stress, 2) inertial oscillations generated by the impulsive nature of the storm passage, 3) the superposition of a large-scale southwesterly flow parallel to the local bathymetry and driven by the cross-shelf pressure gradient, and 4) pressure gradients set up in the water column by the inverse barometer effect of the storm.

5. Summary

Various oceanographic and meteorological data have been presented to demonstrate the impact of Hurricane Andrew on surface and near-surface conditions in the Bahamas, around the coast of Florida, and in the Gulf of Mexico. Sea level pressure, wind direction, wind speed, wind gust, air temperature, wave height, and wave period were strongly influenced by the hurricane at locations within 100 km of the hurricane track. At the Fowey Rocks C-MAN station located just north of the storm track near Miami, maximum sustained winds of 75 m s^{-1} were reported before the instrument failed. Maximum wind speeds of approximately 35 m s^{-1} were observed in the northern Gulf (27.9°N, 90.9°W) at a distance of about 100 km from the storm track. SSTs at buoys 41016 (24.6°N, 76.5°W), 42003 (25.9°N, 85.9°N), and the C-MAN station at 24.5°N, 81.9°W experienced virtually no change during the passage of Andrew. SSTs at the BUSL1 C-MAN station (27.9°N, 90.9°W) on the other hand decreased gradually by up to ~3°C during the first week following the storm, while they decreased by ~2°C at GDIL1 (29.3°N, 90.3°W) within a day and a half following the storm.

During the passage of Andrew, both wave height and wave period increased rapidly to their maximum values as the distance between the storm and buoy 42003 reached its minimum value. The maximum significant wave height was 6.4 m and appears to be a direct response to the wind conditions at the time when the storm center was closest to the buoy location. A maximum wave height of 4.3 m occurred at buoy 42001 prior to the occurrence of the maximum wind speed, which was only ~10 m s^{-1}. The main contribution to the wave field at this point was from swell that arrived from the east. The maximum peak wave period at both buoys 42003 and 42001 was consistently 17 s.

Water levels at the available tide gauges were not strongly affected by the storm in the Bahamas and along most of the east coast of Florida because the core of Andrew in most cases did not pass close to these locations. However, a record high water level was observed at North Miami Beach during passage of the hurricane. Major decreases in water level were observed along the west coast of Florida with a maximum negative surge of −1.2 m occurring at Naples. Maximum (positive) surges of up to +0.5 m occurred at these locations following the passage of Andrew. Increases in water level occurred at several locations along the Gulf coast between the Florida panhandle and Louisiana. For example, a storm surge of +1.2 m was observed at Bay Waveland, Mississippi. Water levels were also higher than historical maxima along the western shore of the lower Mississippi delta.[5]

Current meter data on the coastal shelf close to the hurricane track in the northern Gulf of Mexico (28.4°N, 90.5°W) indicated that current speeds at a

[5] This is true for the tide gage at South Pass, MS, which was installed in 1977. However, water levels were almost certainly higher in this area during Hurricanes Betsy (1965) and Camille (1969).

depth of 1.1 m increased from ~15 cm s^{-1} to almost 140 cm s^{-1} during passage of the storm. Temperature at this location and depth decreased by almost 4°C and salinity increased by 2.0 to 3.0 ppt. Finally, difference maps of satellite-derived SST before and after Andrew (18 to 29 August) showed decreases of 1°–2°C at various locations adjacent to the storm track.

Acknowledgments. The authors would like to thank E. Kalnay for encouraging us to pursue this study, and D. Gilhousen for providing the wind gust data and other NDBC buoy and C-MAN observations that were missing from our files. We particularly thank E. Rappaport for providing the information that we included in the introduction describing the history of Hurricane Andrew. In addition, Rappaport and his colleagues at the National Hurricane Center provided very thorough reviews of the manuscript. The fifth author (NLG) thanks F. Kelly and R. Reid for useful discussions. Current meter data were acquired by the Louisiana Texas Shelf Circulation and Transport Process Study, which is supported by the Minerals Management Service, U.S. Department of Interior. We thank C. Teng for providing the directional wave data that were derived from the wave measurements at the two NDBC buoys in the Gulf of Mexico. We thank S. Lord for providing the surface wind analyses. We thank G. Forristall for additional information and helpful comments. We also thank H. Tolman, S. Lord, D. Rao, and S. Gill for reviewing this manuscript. Finally, we deeply appreciate the very thoughtful and detailed comments from two anonymous reviewers.

REFERENCES

Black, P. G., 1983: Ocean temperature changes induced by tropical cyclones. Ph.D. dissertation, The Pennsylvania State University, 278 pp.

——, R. L. Elsberry, L. K. Shay, R. P. Partridge, and J. D. Hawkins, 1988: Atmospheric boundary layer and oceanic mixed layer observations in Hurricane Josephine obtained from air-deployed drifting buoys and research aircraft. *J. Atmos. Oceanic Technol.*, **5**, 683–698.

Breaker, L. C., L. D. Burroughs, J. F. Culp, N. L. Guinasso Jr., R. L. Teboulle, and C. R. Wong, 1993: Surface and near-surface marine observations during Hurricane Andrew. OPC Tech. Note/NMC Office Note No. 398, 37 pp.

Chang, S., and R. Anthes, 1978: A numerical simulation of the ocean's nonlinear, baroclinic response to translating hurricanes. *J. Phys. Oceanogr.*, **8**, 468–480.

Guinasso, N. L., Jr., Ed., 1992: Field work begins on Gulf oceanography study. *LATEX Fortnightly*, **1**, 2 pp.

Huschke, R. E., Ed., 1959: *Glossary of Meteorology.* Amer. Meteor. Soc., 638 pp.

Kraus, E. B., 1972: *Atmosphere-Ocean Interaction.* Clarendon Press, 275 pp.

McClain, E. P., W. G. Pichel, and C. C. Walton, 1985: Comparative performance of AVHRR-based multichannel sea surface temperature. *J. Geophys. Res.*, **90**, 11 587–11 601.

Meindl, E., 1993: NDBC observations during hurricanes Andrew and Iniki. National Data Buoy Center Tech. Bull. No. 19, 2 pp.

Neumann, C. J., B. R. Jarvinen, A. C. Pike, and J. D. Elms, 1987: *Tropical Cyclones of the North Atlantic Ocean, 1871–1986.* Historical Climatology Series 6-2, NOAA, 186 pp.

National Data Buoy Center, 1989: Technical information sheet—Description of operational payload and hull types used. NDBC, 5 pp. [Available from Engineering Division, National Data Buoy Center, Building 1100, Stennis Space Center, MS 39529.]

——, 1992a: NDBC data platform status report: August 27, 1992–September 3, 1992. NDBC, 10 pp. [Available from National Data Buoy Center, Stennis Space Center, MS 39529-6000.]

——, 1992b: Coastal-Marine Automated Network (C-MAN) NWS Users Guide. NDBC, 55 pp.

National Ocean Service, 1990: Index of tide stations United States of America and miscellaneous other locations. National Ocean Service, NOAA, 122 pp.

Parrish, D. F., and J. C. Derber, 1992: The National Meteorological Center's spectral statistical-interpolation analysis system. *Mon. Wea. Rev.*, **120**, 1747–1763.

Price, J., 1981: Upper ocean response to a hurricane. *J. Phys. Oceanogr.*, **11**, 153–175.

Rappaport, E., 1994: Preliminary report, Hurricane Andrew, August 16–28, 1992. National Hurricane Center, National Weather Service, NOAA, 36 pp.

Robinson, M., R. Bauer, and E. Schroder, 1979: Atlas of North Atlantic–Indian Ocean Monthly Mean Temperatures and Mean Salinities of the Surface Layer. Naval Oceanographic Office, Reference Publication 18, 234 pp.

Schureman, P., 1958: Manual of Harmonic Analysis and Prediction of Tides. Special Publication No. 98 Coast and Geodetic Survey, U.S. Dept. of Commerce, 317 pp.

Swanson, R. C., and G. D. Baxter, 1989: The Bullwinkle platform instrument system. *Proc. 1989 Offshore Technology Conf.*, Houston, TX, 93–100.

Walton, C. C., 1988: Nonlinear multichannel algorithms for estimating sea surface temperature with AVHRR satellite data. *J. Appl. Meteor.*, **27**, 115–124.

World Meteorological Organization, 1981: Manual on the global data-processing system. Vol. 1, Global Aspects, WMO-No. 485, WMO, 106 pp.

Zetler, B., 1982: Computer applications of tides in the National Ocean Survey, Supplement to manual of harmonic analysis and prediction of tides. Special Publication No. 98, National Ocean Service, NOAA, 85 pp.